Hindawi
Advances in Materials Science and Engineering
Volume 2018, Article ID 7401358, 12 pages
https://doi.org/10.1155/2018/7401358

Research Article

Influences on Shotcrete Rebound from Walls with Random Roughness

Zhaoxia Liu,[1,2] Wenhui Bian,[1] Gang Pan,[1,2] Pengcheng Li,[1] and Wenxin Li[1,2]

[1]*College of Mining and Safety Engineering, Shandong University of Science and Technology, Qingdao 266590, China*
[2]*State Key Laboratory of Mining Disaster Prevention and Control Co-founded by Shandong Province and the Ministry of Science and Technology, Shandong University of Science and Technology, Qingdao 266590, China*

Correspondence should be addressed to Gang Pan; threven@sdust.edu.cn

Received 10 June 2018; Revised 5 September 2018; Accepted 27 September 2018; Published 23 October 2018

Academic Editor: Michael Aizenshtein

Concrete slurry can be sprayed on walls for reinforcement; however, there is a certain amount of rebound which is hazardous, lowers production quality, and wastes material. To investigate this problem, we studied single slurry droplets at the mesoscopic level. We deduced the factors influencing droplet spreading and wall adhesion to create models of shotcrete rebound. Then, a numerical simulation orthogonal experiment investigating droplet-wall impacts was performed. The relationship between the spreading coefficient and each influencing factor is discussed, and numerical models are presented. Finally, the obtained models are verified by physical experiments. The results show that the spreading coefficient can be used to better characterize the effect of slurry droplet adhesion to walls. Modeled and experimentally observed droplet-wall impacts showed good consistency. The influence of each factor on the spreading coefficient was determined in the following order of strength: droplet velocity and viscosity, wall roughness, and surface tension. The spreading coefficient increases with velocity, decreases with viscosity and roughness, and increases first and then decreases with surface tension. This study improves the fluid dynamics-based theory of multiphase flow in concrete slurry and provides a theoretical basis for mitigating shotcrete rebound.

1. Introduction

Shotcrete is a building material formed by spraying concrete slurry onto a wall. Shotcrete rebound occurs when the stream of sprayed concrete hits a solid wall and partially bounces off [1]. The rebound phenomenon not only affects the spraying process and wastes concrete but also affects the quality of the project and presents potential safety hazards [2–4]. At present, during the spraying process, many of the operating parameters are determined approximately based on operator experience. The main focus is on the shotcrete materials [5–8], material properties [9–12], and spray equipment [13, 14]. Most existing theoretical studies have investigated aggregate rebound [15–18], while research into the impact of slurry on walls is lacking.

As shown in Figure 1, according to the sprayed concrete spraying process, the jet, adhesion, and deposition process of the shotcrete are divided into three stages. After the material is ejected from the nozzle in the form of a thin stream, the stream is divided into two parts by the action of the air stream: the pure slurry liquid phase and the slurry-wrapped aggregate phase. Among them, the aggregate phase firstly occupies the mortar wrapped on the surface after the wall surface collides with the wall surface. Because there is no cement paste bonding effect, aggregate rebounding is 100%. Some of the slurry is attached to the wall after springback. The slurry phase then reaches the wall and hits the wall alone. Due to the impact force, wall condition, and slurry properties, the slurry droplets are divided into splash rebound, adhesion to the wall, and sliding/loss of adhesion. The slurry that adheres to the wall in the above two stages provides wall adhesion and impact buffering for the subsequent stream. As well, the aggregate particles are gradually deposited from small to large, the subsequent stream is

Figure 1: Using a high-speed camera to capture the jet flow process of shotcrete.

impacted and compacted, and the slurry is adhered to fill the aggregate void. It is evident that the cement paste adhering to the wall is the primary condition for the deposition of the sprayed concrete wall. The cohesive force and impact buffer provided by the cement slurry can significantly reduce the rebound loss of the aggregate. Therefore, it is important to study the rebound of cement slurry for the overall rebound of shotcrete, and doing so would enhance the use of sprayed concrete in engineering applications.

The impingement of slurry spray is a complex process that requires adjustment of many parameters to achieve the best slurry deposition. Due to the impact of slurry on a wall being an unstable process, many phenomena cannot be explained clearly. In the process of investigating this phenomenon, droplets of slurry can be considered as elements in a slurry mass. The behavior of the slurry as it spreads on a wall can be regarded as the sum of multiple droplet impacts. Hence, the dynamics of slurry droplets as they impact a wall need to be studied using multiphase fluid mechanics.

Research into droplets impacting walls is over 100 years old and has two main streams: (1) spreading of droplets as they strike a smooth surface and (2) the spreading of droplets striking a rough wall. The study of droplets spreading on smooth surfaces began in 1877. Worthington [19] used a small experimental platform to study the process of droplets impacting metal planes from different heights. San Marchi [20] used numerical analysis to study the deformation and deposition of single droplets impinging on flat substrates. The recent development of high-speed camera technology has allowed more detailed observations of the morphological changes that occur as a droplet strikes a wall. Zhang [21] used high-speed cameras to capture the impact of Newtonian fluids containing two different surfactants on a solid substrate and analyzed the effect of surfactants on the droplet impact and diffusion processes. Park [22] proposed a hypothesis that droplet diffusion is spherical-shaped and examined the spreading behavior of four fluids at low impact velocity on four different surfaces.

However, there are few studies on droplet spreading on rough wall surfaces. Stow [23] used roughness (Ra) values to characterize the roughness of wall surfaces. The results show that roughness influences droplet impact due to the presence of points on the substrate. The eccentricity caused by anisotropy causes different effects. To make a droplet splash on an inclined panel requires a higher impact velocity than normal. Rioboo [24] analyzed the roughness of several droplets (such as water, alcohol, etc.) in detail. In the wall collision process, droplets get "crushed", and droplet diameter and wall roughness were found to influence this process. However, roughness was characterized by a single parameter, and the experimental error was large and nonrepeatable. Li [25] produced an adjustable pitch columnar array of silicon plates to study the impact of water droplets on silicon plates with regular roughness from an energetic perspective.

The slurry droplet collision process is complicated and affected by both droplet and impact properties [26–29]. In addition, because the sprayed surface is mostly random and rough in the construction process, if the surface is assumed to be an ideal plane and a regular rough surface, the results will be very inconsistent. In order to solve the above-mentioned problems, this paper first establishes a mechanical model of a deviscous sliding wall based on classical mechanics and functional relationships and establishes the connection between the spreading coefficient, wall impact, and drop shape. We model the morphological parameters of a test specimen and simulate slurry-wall impacts by an orthogonal test method. We then discuss the relationship between the spreading factor and its various influences and, finally, verify the applicability and accuracy of the spreading coefficient model via physical experiments.

2. Theoretical Model of Slurry Droplet-Wall Impacts

2.1. Main Form and Classification of the Model. Scholars from various countries have categorized the droplet collision process in order to define different droplet impact models. For example, Bai and Gosman subdivided the collision process into adherence, rebound, spreading, boiling and rupture, rebound with crushing, crushing, and splashing,

according to the shapes of droplets under different conditions [30, 31]. As some of these processes are similar and interchangeable, they are further classified on the basis of predecessors to the collision process. Liu and Xu proposed that the processes are analogous to a spring-mass system; the process of droplet-wall impact can be divided into three stages: rebound, crushing, and adhesion [32]. Stanton assumed there to be a liquid film on the wall and considered only four impact modes: adhesion, spreading, rebound, and splashing [33]. In this paper, it is the standard for whether rebound of slurry droplets striking a wall during the spraying of shotcrete, and droplet-wall impacts are divided into three categories according to the tendency of droplets to move against the wall. As shown in Figure 2, these categories are as follows: splash rebound, adhesion to the wall, and sliding/loss of adhesion. Among them, adhesion to the wall is the one we hope for in shotcrete.

The rebound of cement paste after striking a wall generally has two components. Firstly, the slurry loss caused by crushing, spattering, and rebound of slurry droplets is defined as *splash rebound* and is generally influenced by collision velocity, inertial force, or the absolute dominant influence of gas vorticity [34, 35]. Secondly, slurry loss due to slurry not fully spreading on a wall is defined as sliding/loss of adhesion.

Because slurry does not get fully spread during low-velocity wall collision, the smaller the relative contact area is, the smaller the adhesion force is. The slurry seat is generally spherical, and the center of gravity is away from the wall surface, resulting in debonding and sliding of the slurry. In order to solve the above problem, a spreading coefficient D′ (the ratio of the spread diameter to the initial diameter at equilibrium) is defined to represent the droplet's form and the effect of wall adherence after slurry impact. The following will be based on the classical mechanics: study the effect of spreading coefficient on the rebound of the slurry wall and find the factors that affect the spreading coefficient.

2.2. Analysis of the Main Factors Affecting the Spreading Coefficient. According to the actual situation in the experiment, the shape of slurry droplets sprayed onto a rock wall is approximately hemispherical (Figure 3(a)). The geometric model of droplet adhesion after impact is shown in Figure 3(b). The height of the spherical crown is defined as H and the radius is R.

When the slurry is sprayed at a certain velocity, the slurry droplets adhere to the wall surface as spherical crowns. From the mechanical point of view, when the spreading coefficient is larger, the moment generated by the force of gravity and fluid tangential friction force is less likely to lower adhesion, and the droplets firmly adhere to the rock wall surface. The attachment surface is circular. When the slurry spreading coefficient reaches a critical value, the upper part of the slurry (MM′, Figure 3) first breaks away from the wall surface, the slurry rolls along the wall surface, and the lower part (NN′, Figure 3) readheres. However, due to the resultant forces at the new position, the droplet still breaks adhesion and the slurry continues to roll off until it comes off the wall.

The descent distance of the first arrival of the critical spread coefficient is ds, and the descent area is dA (the crescent portion in Figure 3). Then, the work of gravity in this process, represented by $p \cdot ds$, overcomes the stickiness. The work done by the attaching force is $W_a \cdot dA$, and the work done by viscous friction is $\mu \cdot dv/ds \cdot da$. The free enthalpy lost when a new adhesive interface is generated is negligibly small, and the work balance relationship is

$$P \cdot ds = W_a \cdot dA + 2C_k \cdot \mu \frac{dv}{ds} \cdot ds \cdot R. \tag{1}$$

In the formula, the correction coefficient of the friction force, which is a constant, is determined by the wall surface roughness.

The volume of the slurry is $V = 1/6 \cdot \pi \cdot H(3R^2 + H^2)$ and the spherical cap, $H = R \cdot \tan\theta$, is substituted into the above formula:

$$V = \frac{\pi R^3}{6} \tan\theta \left(3 + \tan^2\theta\right). \tag{2}$$

After reaching the debonding radius, the distance of each debonding and sliding action is S. The corresponding sliding area dA can be obtained by analytical methods. As shown in Figure 2(c), the orthogonal coordinate system is established with the O' center of the sliding center as the origin. Then, the analytical formulae for the circles O and O' are

$$\begin{aligned} x^2 + (y - s)^2 &= R^2, \\ x^2 + y^2 &= R^2. \end{aligned} \tag{3}$$

The coordinates of k at the intersection of the above formulae are $x = \sqrt{R^2 - (s^2/4)}$; $y = s/2$.

The area enclosed in the first quadrant is A_1, A_2, according to the definite integral knowledge:

$$\begin{aligned} A_1 &= \int_0^{\sqrt{R^2-(s^2/4)}} \left(\sqrt{R^2 - x^2} + s\right) dx, \\ A_2 &= \int_0^{\sqrt{R^2-(s^2/4)}} \sqrt{R^2 - x^2}\, dx. \end{aligned} \tag{4}$$

As shown in Figure 3(c), there is a relationship between the area of the shaded region and the sliding distance: when s tends to zero, the area tends to zero, so this part is negligible.

$$dA = 2\left(A_1 - A_2\right) = 2\int_0^{\sqrt{R^2-(s^2/4)}} s\, dx = 2\, ds \cdot \sqrt{R^2 - \left(\frac{ds^2}{4}\right)}. \tag{5}$$

In terms of magnitude, due to $R^2 \gg ds^2/4$, then $dA \approx 2ds \cdot R$.

So, the work balance equation can be written as

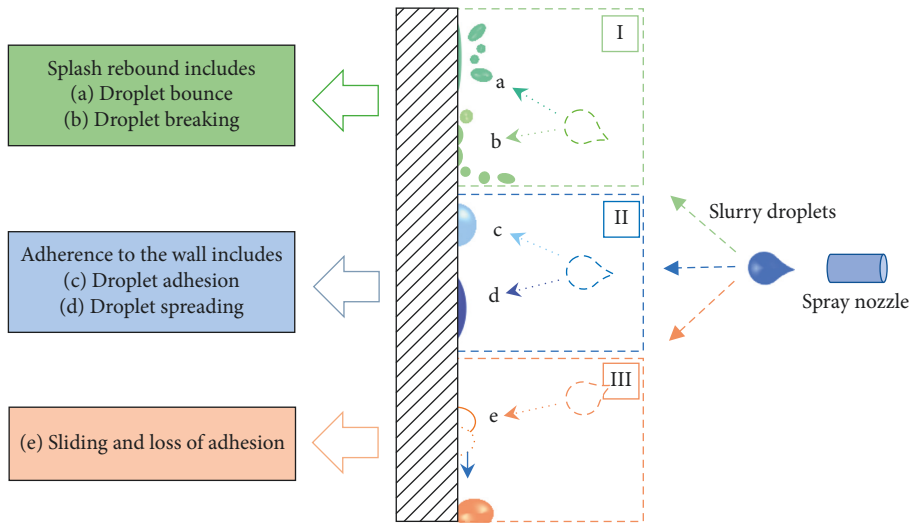

Figure 2: Classification of slurry droplet impacts on a wall: (I) splash rebound, (II) adhesion to the wall, and (III) sliding and loss of adhesion.

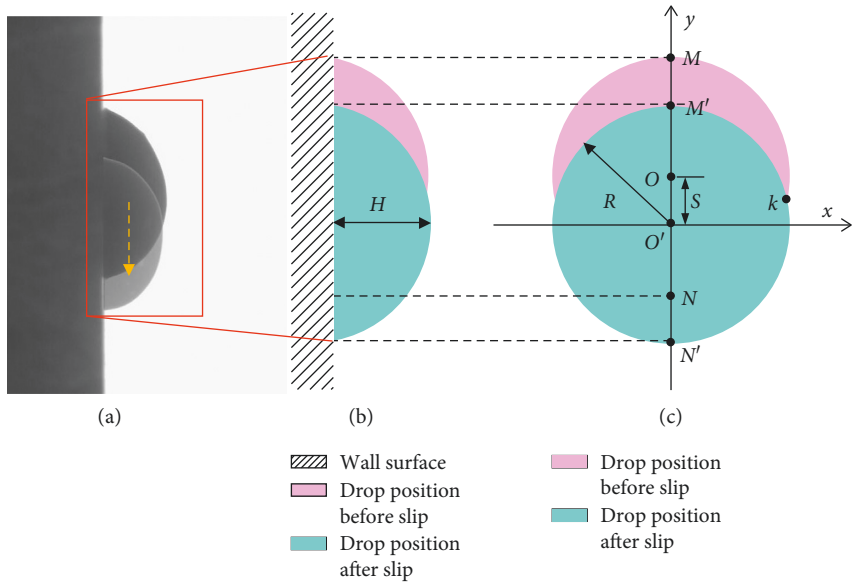

Figure 3: Droplet on a wall sliding/losing adhesion. (a) Real slurry sliding away from the wall and losing adhesion. (b) Slide away from wall and lose adhesion model. (c) Analytical geometry of the model.

$$\frac{\pi\varphi g R^3}{6}\tan\theta\left(3+\tan^2\theta\right)\cdot ds = e_{lv}\left(1+\cos\theta\right)\cdot 2\,ds \cdot R + 2C_k\cdot\mu\frac{dv}{ds}\cdot ds\cdot R. \tag{6}$$

The slurry droplet radius is

$$R=\left[\frac{12\sigma\left(1+\cos\theta\right)ds + C_k\cdot\mu\cdot dv}{\pi\varphi g\tan\theta\left(3+\tan^2\theta\right)ds}\right]^{1/2}. \tag{7}$$

Assuming that the initial diameter of the droplet is D_0, the relationship between the spreading coefficient D' and the droplet radius R is $D' = 2R/D0$.

The spreading coefficient D' is

$$D' = \frac{2}{D_0}\left[\frac{12e_{lv}\left(1+\cos\theta\right)ds + C_k\cdot\mu\cdot dv}{\pi\varphi g\tan\theta\left(3+\tan^2\theta\right)ds}\right]^{1/2}. \tag{8}$$

The above analysis shows that surface tension, contact angle, roughness, viscosity, velocity, and density all affect the spreading coefficient. There is a correspondence between the surface tension of the liquid and the contact angle, so the surface tension can be studied alone [36]. Secondly, the millimeter droplet density changes very little, so density has negligible influence on the spreading coefficient.

3. Slurry-Wall Impact Simulation and Orthogonal Test

In order to quantitatively study the effects of surface properties, impact properties, and droplet properties on

slurry spreading during wall impact, COMSOL Multiphysics software was used for mathematical modeling and numerical simulation analysis. COMSOL Multiphysics is a numerical simulation software based on the finite element method. It can realize multiphysics coupling calculations by solving partial differential equations, which reflect the most basic scientific principles and their two-phase flow level. The set physics interface simulates the motion of a droplet impacting a solid surface.

3.1. Selection of Control Equations. The model simulates fluid mass and momentum transfer based on the Navier–Stokes equation for incompressible fluids. The effects of surface tension must also be included in the model. Therefore, the Navier–Stokes equation is

$$\rho\left(\frac{\partial u}{\partial t} + u \cdot \nabla u\right) = -\nabla p + \nabla \cdot \mu\left(\nabla u + \nabla u^{T}\right) + \rho g + F_{\mathrm{st}},$$
$$\nabla \cdot u = 0. \tag{9}$$

In the formula, u is the velocity field (m/s); ρ is density (kg/m^3); p is pressure (Pa); μ is viscosity (mPa.s); ρg is gravity; and F_{st} is surface tension.

3.2. Establishment of Geometric Models and Selection of Boundary Conditions. In order to facilitate numerical simulation, the dynamic process of a single slurry droplet impacting a surface with random roughness at low velocity can be simplified as follows. A slurry droplet in the atmosphere with a certain initial velocity is located directly above the rough surface. Wall roughness is modeled according to the actual topographic parameters of the experimental substrate. The numerical simulation uses a 30 mm × 50 mm calculation area. The entire physical model is shown in Figure 4.

At the same time, due to the complex motion of droplets in the computational domain, some reasonable assumptions have been made to simplify the calculations. (1) The fluid is incompressible during movement; (2) the surface tension of the fluid is constant during the collision process; (3) there is no change in the contact angle within a surface of consistent roughness; and (4) there is no phase change at the gas-liquid interface, nor any fluid heat transfer.

The open boundary condition of the upper boundary of the model can be used to achieve the free entry and exit of air. The left and right boundaries of the model are pressure exit boundaries, and the air velocity is 0. The lower boundary of the model is the boundary condition of the wetting wall. At the same time, during the numerical simulation calculations, it was found that adding the initial velocity directly did not converge the calculation result. The reason was that there was a sudden change in the value. By defining the volume force, the collision velocity can reach the set value, and the above calculation is not solved [37]. There is a problem of convergence, expressed as

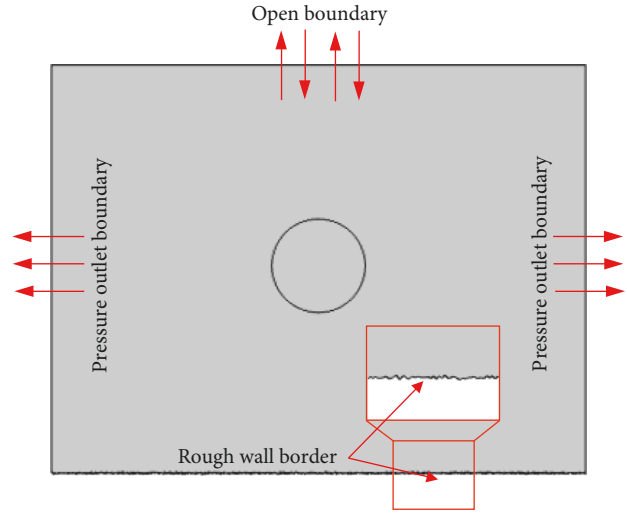

Figure 4: Physical model of droplet-wall interaction.

$$F_v = -tpf1.rho2 * \left(v\_in^2/2/h\_in - g\_const\right) * tpf1.Vf2 * (t <= t\_in). \tag{10}$$

The parameters in the formula are software-preset variables, where $tpf1.rho2$ refers to droplet density; v_in is the velocity; h_in is the drop height; g_const is gravitational acceleration; $tpf1.Vf2$ is the droplet volume fraction; t_in is the drop time; and $t <= t\_in$ means only the volume force exists in the falling process. After the droplet hits the wall, the volume force disappears.

3.3. Orthogonal Test. Several factors influence the spreading coefficient described in Equation (10). In order to further analyze their influence, the numerical simulation method described in Section 3.2 is used. The surface tension, viscosity, wall roughness, and velocity of impact are orthogonal experimental factors. The spreading coefficient after the liquid droplet impacts the wall is an orthogonal test index, and the L_9 (3^4) orthogonal table is used to perform four factors and three levels of orthogonality. Tests and orthogonal test factor levels are shown in Table 1.

Orthogonal tests and numerical simulation results are shown in Table 2 and Figure 5.

Analysis of Orthogonal test results by range analysis. Range analysis is a visual analysis method that assesses the extent of the effect by analyzing the range of range R. If X_{ij} represents i levels of j factors and Y_{ij} represents the result of X_{ij}, then the range R is calculated as follows [38]:

$$k_{ij} = \sum_{k=1}^{s} \frac{Y_{ijk}}{S} \quad (i = 1, 2, 3, \ldots, \ j = A, B, C, \ldots),$$
$$R_j = \max\left\{k_{1j}, k_{2j}, \ldots, k_{rj}\right\} - \min\left\{k_{1j}, k_{2j}, \ldots, k_{rj}\right\}. \tag{11}$$

Here, R_j represents the range of j factors. The increase of R_j indicates that the influence of j factors is more important. Variable s is the number of values, and r is the level of factors.

Table 1: Orthogonal design parameters.

Factor	Level
Surface tension (mN/m)	6.3, 8, 10.5
Viscosity (mPa.s)	53, 97, 135
Roughness (Ra, μm)	0.5, 1.5, 2.5
Velocity (m/s)	1, 2, 4

Statistical analysis software (SPSS) was used to perform the range analysis on the orthogonal test data. According to the range analysis results (Table 3), the order of influence of the factors, from strong to weak, is velocity, viscosity, roughness, and surface tension.

3.3.1. Variation of Spreading Coefficient and Influencing Factors. Using SPSS, the least significant difference method (LSD) was used to conduct post hoc multiple comparison analysis to obtain the single factor marginal mean value of the estimated spread coefficient, as shown in Figure 6. Postmortem multiple analysis is a common method for obtaining information from data; its basic principle is to use a critical difference to test each pair of means. If the difference between a pair of means is greater than the critical difference, they are considered to be significantly different. The LSD method is a multiple comparison method proposed by Fisher in 1935. Using t-tests to conduct pairwise comparison between the groups has the advantage of high sensitivity of detection, such that small differences between means may also be tested [39–41].

From Figure 6, we can see the following relationships:

(1) The spreading coefficient increases first and then decreases with surface tension. There is a sudden change in the value. There are two stages of spreading and retraction in the stage of droplet impact. The surface tension provides resistance during the spreading stage and provides force during the retraction stage. The surface tension of 6.3–8 mN/m is relatively small, and the resistance during spreading is small, leading to a gradual increase in the spreading coefficient. When the surface coefficient is gradually increased to about 10.5 mN/m, the spreading resistance is large and the droplets are difficult to spread. The greater the power of the retraction phase, the smaller the spreading coefficient.

(2) The spreading coefficient is negatively correlated with viscosity and wall roughness. That is, the spreading coefficient decreases with increasing viscosity and wall roughness. This is because viscosity and wall roughness provide resistance over the entire process of droplet-surface collision.

(3) The spreading coefficient increases with velocity. The literature [37] also reports similar conclusions from experiments of collisions between Newtonian and non-Newtonian fluids at room temperature. The inertial force caused by velocity is significantly larger than the other influences by an order of magnitude.

(4) It can be seen from the trendline of the graph that within the range studied, the spreading coefficient has a tendency to increase with velocity and decrease with increasing surface tension, viscosity, and surface roughness.

3.3.2. Expression of Factors Influencing the Spreading Coefficient. According to Figure 6, a single factor is used to estimate the marginal mean value of the spreading coefficient. SPSS was used to carry out a one-dimensional regression analysis, and mathematical equations of the spreading factor and individual influencing factors were derived to obtain Equations (12) to (15):

$$D' = -0.0255\sigma^2 + 0.4116\sigma + 0.6788, \tag{12}$$

$$D' = -0.0069\mu + 2.9294, \tag{13}$$

$$D' = -0.095F_{\mathrm{Ra}} + 2.4192, \tag{14}$$

$$D' = -0.0517V^2 + 0.765V + 0.8267. \tag{15}$$

In the formulae, σ is surface tension (mN/m); μ is viscosity (mPa.s); F_{Ra} is wall surface roughness (μm); and V is velocity (m/s).

From Equations (12) to (15), the spreading factor can be expressed as a linear function of viscosity and roughness and a quadratic function of surface tension and velocity. Therefore, a multivariate regression analysis was conducted and Equation (16) was used to express the relationship between the spreading factor and various influencing factors.

$$D' = k_{11}V^2 + k_{12}V + k_{21}\sigma^2 + k_{22}\sigma + k_{31}\mu + k_{41}F_{\mathrm{Ra}} + k_{51}, \tag{16}$$

where k_{ij} is a constant.

Matlab software was used to make Equation (16) fit the orthogonal experimental results of Table 2 to obtain Equation (17):

$$\begin{aligned} D' &= -0.04833V^2 + 0.74833V - 0.02017\sigma^2 + 0.31978\sigma \\ &\quad - 0.00663\mu - 0.08167F_{\mathrm{Ra}} + 0.3937, \\ R^2 &= 0.99139. \end{aligned} \tag{17}$$

In order to verify the accuracy of the above numerical simulation and the rationality of the influencing factors on the spreading factor, a different combination with orthogonal testing was selected, and the obtained function was verified by a physical experiment.

4. Droplet Impact Physical Experiment

4.1. Experiment Preparation

4.1.1. Experimental Substrate. Experimental substrate was taken from the Tangkou Coal Mine of the Zibo Mining

Table 2: Orthogonal tables and range analysis results.

Experiment no.	Surface tension (mN/m)	Viscosity (mPa.s)	Roughness (Ra, μm)	Velocity (m/s)	Spreading coefficient
1	6.3	53	0.5	1	1.89
2	6.3	97	1.5	2	2.2
3	6.3	135	2.5	4	2.7
4	8	53	1.5	4	3.4
5	8	97	2.5	1	1.55
6	8	135	0.5	2	2
7	10.5	53	2.5	2	2.25
8	10.5	97	0.5	4	3.1
9	10.5	135	1.5	1	1.2

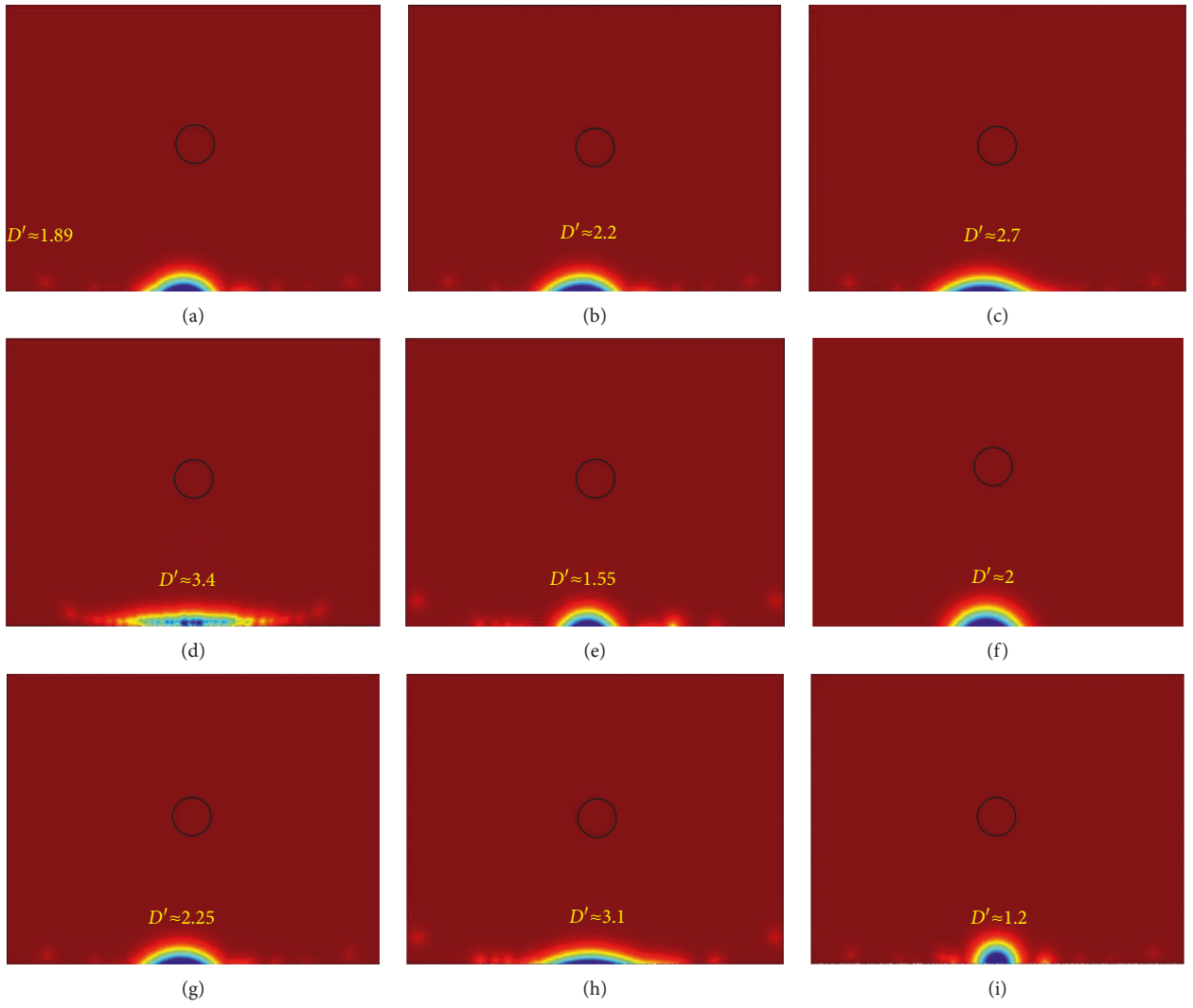

Figure 5: Orthogonal experimental simulation results.

Group. The specific location was a rock formation in the 1–2 track alley where a wet spray operation was being performed on the 630 track main roadway. In order to ensure the consistency of the raw material's composition, the experimental substrates were all taken from the same stone. First, the stones were cut into 50 mm × 50 mm × 10 mm cubes, then 500–7000 CW sandpaper was used to Polish them on a p-2 metallographic polishing machine. Afterwards, they were washed with detergent and pure water. Finally, they were put in a 99.5% mass fraction ethanol solution and subjected to ultrasonic vibration for 1 h.

Before the experiment, the surfaces of the substrates were blown dry with nitrogen, and the morphology of the substrate was measured using a Leica DCM8 (Leica DCM, Germany), as shown in Figure 7(a). A surface roughness measuring instrument (TR200, China) was used to measure

Table 3: Range analysis results.

	Surface tension (mN/m)	Viscosity (mPa.s)	Roughness (Ra, μm)	Velocity (m/s)
K1	2.263	2.513	2.330	1.547
K2	2.317	2.283	2.267	2.150
K3	2.183	1.967	2.167	3.067
R	0.134	0.546	0.163	1.520
PSF		V > μ > Ra > σ		

Note. PSF = primary and secondary factors; K is the sum of the test results corresponding to the horizontal number i on any column; R = max{K1, K2, K3} −min{K1, K2, K3}.

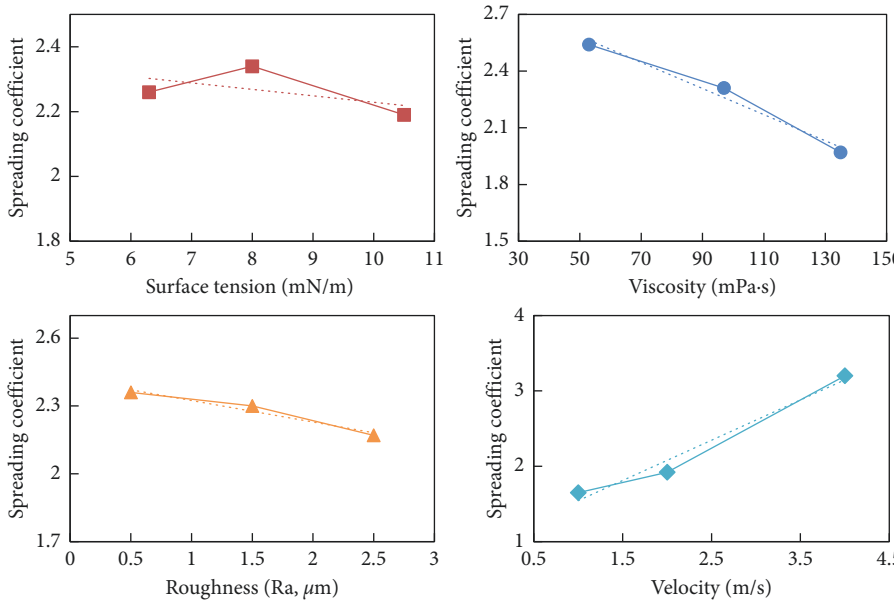

Figure 6: Relationships between marginal means and factors influencing the spreading coefficient.

surface roughness, as shown in Figure 7(b). Multiple measurements were made to obtain an average center position roughness value R_a (solid surface roughness thickness RMS value) and the roughness value W_r (the ratio of the actual contact length to the horizontal projection length). Matlab programming based on two one-dimensional topological parameters was used to construct two-dimensional parametric lines to provide a roughness value based on the real specimen's surface for numerical simulation. The reconstruction results are shown in Figure 7(c). At the same time, in order to prevent the occurrence of two roughness obscurations in the course of the numerical simulations and experiments, uniform roughness values were used to represent the same substrate [37].

4.1.2. Experimental Materials. We used standard PO42.5 cement (China United Cement Corporation) with a water to cement ratio of 1 : 2. Table 4 shows the basic properties of the cement slurry. The composite modified CR-I viscosity reducer significantly improved the viscosity of the slurry [42], using a concrete rotary rheometer (eBT-2, Germany) to measure viscosity changes at different levels. Modified lignosulfonate can vary the surface tension of the slurry without affecting its other properties greatly [43, 44], and a surface tension meter (KRUSS-K12, Germany) was used to measure the surface tension changes at different dosages. Figure 8 shows the curves of viscosity and surface tension vs additions of different amounts of viscosity reducer and modified lignosulfonate.

4.2. Experimental System. As shown in Figure 9, in the experiment, a high-speed video camera (Phantom VRI, USA) was used to record droplets falling and impacting the substrate. The camera used a frame rate of 1000 frames per second and a resolution of 1024 × 512 pixels. During the experiment, the camera was tilted and leveled. The included angle was approximately 30°, and the droplet impact process was photographed within the measurement area. The images were transmitted to a computer through a data acquisition system. A single drop generator was connected to a syringe using a syringe pump (top-5300, Japan) with a flow rate of 33.5 ml·h^{-1}. The diameter of the droplets produced was related to the outer diameter of the injection port of the syringe, which was 2 mm. The theoretical initial diameter of the droplet was approximately 3.7 mm. The theoretical diameter was measured by weighing 200 drops and calculating the mean diameter according to mass/volume relationships. The mean droplet diameter was calculated as 4 mm, which was used as the initial diameter of the droplets used in the experiments. The mean velocity of a droplet just before it

(a) (b) (c)

Figure 7: Experimental substrate morphology measurement and reconstruction. (a) Substrate topography measurement. (b) Substrate roughness measurement. (c) Substrate topography reconstruction results.

Table 4: Basic properties of the grout used.

W/C (w%)	Viscosity (mPa.s)	Surface tension (mN/m)	Density (g/cm^3)	Gelation time	
				Initial setting	Final setting
1 : 2	135	10.5	1.82	7 h 40 min	11 h 32 min

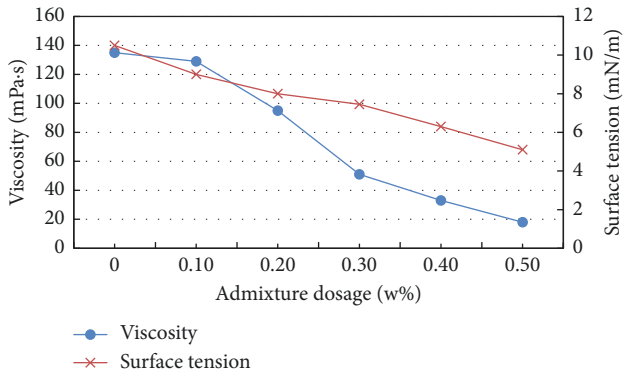

Figure 8: Viscosity and surface tension curves with different amounts of viscosity reducer and modified lignosulfonate.

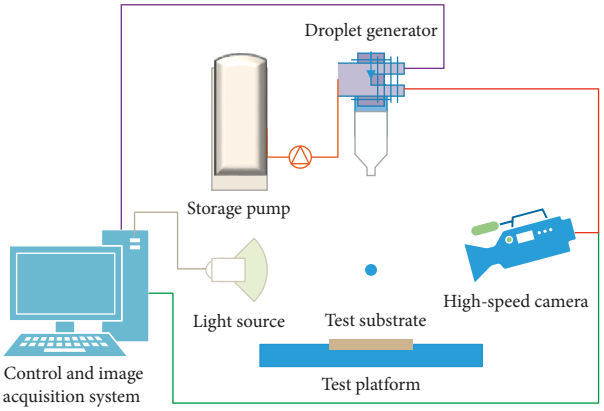

Figure 9: Schematic diagram of the single-drop substrate impact test system.

struck the substrate was 0.2 m/s. The impact velocity was controlled with a range of 1–4 m/s with an error of ±0.02 m/s.

4.3. Experimental Results. To verify Equation (17), according to the combinations in orthogonal Table 2, various combinations of values of surface tension, viscosity, roughness, velocity, and other factors were selected for the droplet-substrate impact tests. The tests and various spread coefficient sizes are shown in Figure 10. The spreading coefficient of each group was obtained, and the results were compared with the spreading coefficient model shown in Table 5.

Table 5 shows that the mean relative error between the experimental and theoretical data was 3.65%, with a range of 0.3%–6.3%. It shows that the influence factor expression of spreading coefficients can better quantify the effect of viscosity, surface tension, roughness, and velocity on the spreading coefficient.

5. Conclusions

(1) By means of mechanical analysis, spreading coefficients were used to characterize the effect of slurry droplet-wall adhesion, allowing the derivation of a formula for spreading coefficient based on the influential factors. The key factors influencing the impact and adhesion of slurry on a wall are droplet velocity and viscosity, wall roughness, and surface tension.

(2) Through numerical simulation and based on the results of an orthogonal experiment, a model of the spreading coefficient was derived. It quantitatively characterizes the relationship between the spreading coefficient and its influencing factors, thereby achieving the transition from qualitative theoretical research to quantitative experimental research. From the expression's constants for the influencing factors, it can be seen that velocity (constant = 0.74833) has a significant effect on the spreading coefficient. Since

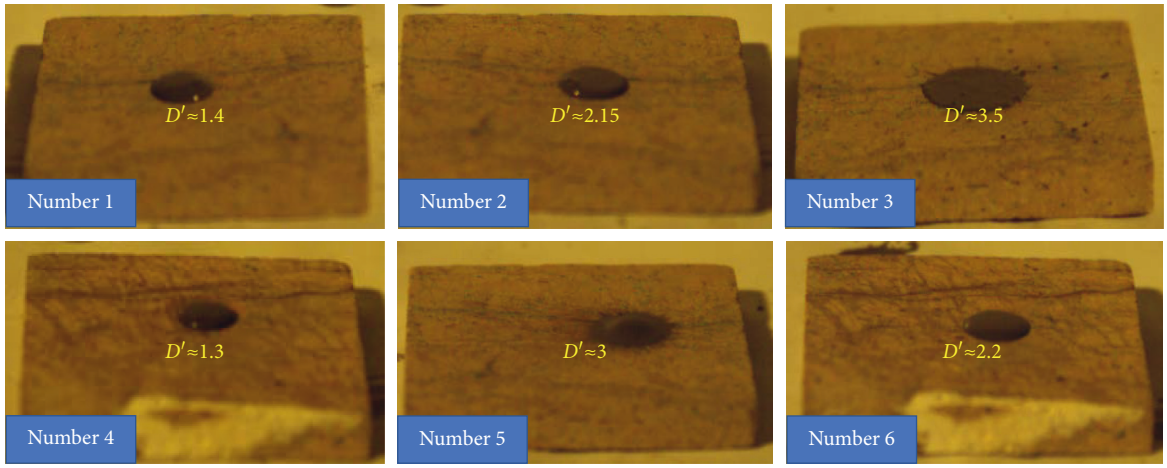

Figure 10: Droplet spreading after striking the substrate of the test apparatus.

Table 5: Experimental verification of spreading coefficients.

Test no.	Surface tension (mN/m)	Viscosity (mPa.s)	Roughness (μm)	Velocity (m/s)	Spreading coefficient		RE (%)
					EV	TV	
1	6.3	135	0.5	1	1.40	1.37	2%
2	6.3	97	2.5	2	2.15	2.06	4%
3	8	53	0.5	4	3.50	3.49	0.3%
4	8	135	1.5	1	1.30	1.34	3.4%
5	10.5	53	2.5	4	3.02	3.19	6.3%
6	10.5	97	1.5	2	2.21	2.07	5.9%

EV = experimental value; TV = theoretical value; RE = relative error.

the droplet size (5 mm) was much larger than the range of the roughness (0.5–2.5 μm), at the low velocity used in this study, roughness was also an important determinant of the spreading coefficient.

(3) Through physical droplet-wall impact tests, a numerical simulation of the factors affecting the spreading coefficient was validated. The experimental and theoretical values were in good agreement, and a further explanation was given based on the actual morphological parameters. A random wall roughness model can best represent the rough surface morphology of real walls.

At present, experimental research into the rebound of wet sprayed concrete slurry is relatively rare and its mechanisms are poorly understood. Therefore, the rebound mechanism requires further extensive theoretical and experimental research.

6. Discussion

This paper combines the stage division of shotcrete jets used in engineering practice and, from a phenomenological perspective, creatively proposes the problem of slurry rebound. Furthermore, based on the fact that slurry acts as a binder in shotcrete, it is recognized that the rebound loss of slurry plays an important role in shotcrete's overall rebound characteristics. This paper focuses on the sliding and loss-of-adhesion mechanisms of slurry rebound. The critical conditions of detachment adhesion are applied not only for vertical walls but also for horizontal top walls, which provides a theory for describing slurry rebound. At the same time, a linear relationship between slurry impact and spreading on a rough wall is obtained. This provides information for the optimization of shotcrete parameters and mixtures. It is conceivable that an admixture could be created that changes the viscosity and surface tension of shotcrete to reduce rebound.

As for future work to be done for this study, other types of slurry rebound losses should be studied first. Secondly, there are many factors influencing the behavior of slurry. From the rheological properties of the slurry, the yield stress is introduced as an input parameter, and the difference between using yield stress and interface adhesion as the critical condition should be determined. In addition, after considering all the influencing parameters, an admixture should be developed that results in significantly less rebound than existing shotcrete mixtures.

In summary, experimental research into the rebound of wet sprayed concrete slurry is relatively rare and its mechanisms are poorly understood. Therefore, the rebound mechanism requires extensive theoretical and experimental research.

Data Availability

The data used to support the findings of this study are available from the corresponding author upon request.

Conflicts of Interest

The authors declare that they have no conflicts of interest.

Acknowledgments

This work was supported by the National Key Research and Development Plan of the 13th Five-Year Period (2017YFC0805203), the National Natural Science Foundation of China (51604163), and the Applied Research Project Foundation of Qingdao Postdoctoral Researchers (201576).

References

[1] GB 50086-2015, *Technical Code for Engineering of Ground Anchorages and Shotcrete Support*, Chinese Standard Press, Beijing, china, 2015.

[2] H. S. Armelin, N. Banthia, D. R. Morgan et al., "Rebound in dry-mix shotcrete," *Concrete International*, vol. 19, 1997.

[3] J. Kaufmann, K. Frech, P. Schuetz et al., "Rebound and orientation of fibers in wet sprayed concrete applications," *Construction and Building Materials*, vol. 49, no. 6, pp. 15–22, 2013.

[4] H. S. Armelin, *Rebound and toughening mechanisms in steel fiber reinforced dry-mix shotcrete*, The University of Columbia, New York, NY, United States, 1997.

[5] J. P. Won, U. J. Hwang, C. K. Kim et al., "Mechanical performance of shotcrete made with a high-strength cement-based mineral accelerator," *Construction and Building Materials*, vol. 49, no. 12, pp. 175–183, 2013.

[6] K. K. Yun, S. Y. Choi, and J. H. Yeon, "Effects of admixtures on the rheological properties of high-performance wet-mix shotcrete mixtures," *Construction and Building Materials*, vol. 78, pp. 194–202, 2015.

[7] J. Pickelmann and J. Plank, "A mechanistic study explaining the synergistic viscosity increase obtained from polyethylene oxide (PEO) and β-naphthalene sulfonate (BNS) in shotcrete," *Cement and Concrete Research*, vol. 42, no. 11, pp. 1409–1416, 2012.

[8] P. Choi, J. H. Yeon, and K. K. Yun, "Air-void structure, strength, and permeability of wet-mix shotcrete before and after shotcreting operation: the influences of silica fume and air-entraining agent," *Cement and Concrete Composites*, vol. 70, pp. 69–77, 2016.

[9] K. K. Yun, P. Choi, and J. H. Yeon, "Correlating rheological properties to the pumpability and shootability of wet-mix shotcrete mixtures," *Construction and Building Materials*, vol. 98, pp. 884–891, 2015.

[10] P. Choi, K. K. Yun, and J. H. Yeon, "Effects of mineral admixtures and steel fiber on rheology, strength, and chloride ion penetration resistance characteristics of wet-mix shotcrete mixtures containing crushed aggregates," *Construction and Building Materials*, vol. 142, pp. 376–384, 2017.

[11] P. Choi, K. K. Yun, and J. H. Yeon, "Rheological properties of wet-mix shotcrete mixtures made with crushed aggregate," *Journal of Materials in Civil Engineering*, vol. 29, no. 11, article 04017227, 2017.

[12] R. G. Pileggi, Y. A. Marques, D. V. Filho et al., "Aditivos para concretos de projeção WET-Shotcrete Additives," *Cerâmica*, vol. 48, no. 308, pp. 199–205, 2002.

[13] J.-D. Lemay, M. Jolin, and R. Gagné, "Ultra rapid strength development in dry-mix shotcrete for ultra rapid support in challenging mining conditions. Deep mining 2014," in *Proceedings of 7th International Conference on Deep and High Stress Mining*, Australian Centre for Geomechanics, Nedlands, Australia, September 2014.

[14] N. Ginouse, M. Jolin, and B. Bissonnette, "Effect of equipment on spray velocity distribution in shotcrete applications," *Construction and Building Materials*, vol. 70, no. 70, pp. 362–369, 2014.

[15] D. Beaupre and M. Jolin, "Effects of particle-size distribution in dry process shotcrete," *Aci Materials Journal*, vol. 101, no. 2, pp. 131–135, 2004.

[16] H. S. Armelin and N. Banthia, "Mechanics of aggregate rebound in shotcrete—(Part I)," *Materials and Structures*, vol. 31, no. 2, pp. 91–98, 1998.

[17] H. S. Armelin and N. Banthia, "Development of a general model of aggregate rebound for dry-mix shotcrete—(Part II)," *Materials and Structures*, vol. 31, no. 3, pp. 195–202, 1998.

[18] H. S. Armelin, N. Banthia, and D. R. Morgan, "Particle kinematics in dry-mix shotcrete–research in progress," *Sprayed Concrete Technology*, vol. 27, p. 243, 1996.

[19] A. M. Worthington III, "A second paper on the forms assumed by drops of liquids falling vertically on a horizontal plate," *Proceedings of the Royal Society of London*, vol. 25, no. 171–178, pp. 498–503, 1877.

[20] C. San Marchi et al., "Numerical analysis of the deformation and solidification of a single droplet impinging onto a flat substrate," *Journal of Materials Science*, vol. 28, no. 12, pp. 3313–3321, 1993.

[21] X. Zhang and A. B. Osman, "Dynamic surface tension effects in impact of a drop with a solid surface," *Journal of Colloid and Interface Science*, vol. 187, no. 1, pp. 166–178, 1997.

[22] H. Park, W.W. Carr, J. Zhu, and J. F. Morris, "Single drop impaction on a solid surface," *AIChE journal*, vol. 49, no. 10, pp. 2461–2471, 2003.

[23] C. D. Stow and M. G. Hadfield, "An experimental investigation of fluid flow resulting from the impact of a water drop with an unyielding dry surface," *Proceedings of the Royal Society A: Mathematical, Physical and Engineering Sciences*, vol. 373, no. 1755, pp. 419–441, 1981.

[24] R. Rioboo, T. Cameron, and M. Marengo, "Outcomes from a drop impact on solid surfaces," *Atomization and Sprays*, vol. 11, no. 2, 2001.

[25] X. Li, L. Mao, and X. Ma, "Dynamic behavior of water droplet impact on microtextured surfaces: the effect of geometrical parameters on anisotropic wetting and the maximum spreading diameter," *Langmuir*, vol. 29, no. 4, pp. 1129–1138, 2013.

[26] B. A. Dwiyantoro, "Capillary effects during droplet formation on the solid surface," *Advanced Materials Research*, vol. 683, pp. 889–893, 2013.

[27] K. L. Pan, K. C. Tseng, and C. H. Wang, "Breakup of a droplet at high velocity impacting a solid surface," *Experiments in Fluids*, vol. 48, no. 1, pp. 143–156, 2010.

[28] B. L. Scheller and D. W. Bousfield, "Newtonian drop impact with a solid surface," *AIChE Journal*, vol. 41, no. 6, pp. 1357–1367, 2010.

[29] R. Crooks, J. Cooper-White, and D. V. Boger, "The role of dynamic surface tension and elasticity on the dynamics of drop impact," *Chemical Engineering Science*, vol. 56, no. 19, pp. 5575–5592, 2001.

[30] C. Bai and A. D. Gosman, "Development of methodology for spray impingement simulation," SAE Technical Paper, Report no. 950283, 1995.

[31] C. X. Bai, H. Rusche, and A. D. Gosman, "Modeling of gasoline spray impingement," *Atomization and Sprays*, vol. 12, no. 1–3, pp. 1–28, 2002.

[32] H. Xu, Y. Liu, P. He et al., "The TAR model for calculation of droplet/wall impingement," *Journal of Fluids Engineering*, vol. 120, no. 3, pp. 593–597, 1998.

[33] D. W. Stanton and C. J. Rutland, "Modeling fuel film formation and wall interaction in diesel engines," SAE Technical Paper, 1996.

[34] C. Mundo, M. Sommerfeld, and C. Tropea, "Droplet-wall collisions: experimental studies of the deformation and breakup process," *International Journal of Multiphase Flow*, vol. 21, no. 2, pp. 151–173, 1995.

[35] C. Mundo, C. Tropea, and M. Sommerfeld, "Numerical and experimental investigation of spray characteristics in the vicinity of a rigid wall," *Experimental Thermal and Fluid Science*, vol. 15, no. 1, pp. 80–86, 1980.

[36] H. Y. Erbil, *Surface Chemistry: Of Solid and Liquid Interfaces, Surface chemistry of solid and liquid interfaces*, Wiley-Blackwell, Hoboken, NJ, USA, 2006.

[37] H. Zhang, "Study on spreading dynamics of droplets on random rough surface," MS thesis, Suzhou University, Jiangsu, China, 2015.

[38] X. M. Zhao, *Experimental Design Method*, Science Press, Beijing, China, 2006.

[39] G. Keppel, *Design and Analysis: A Researcher's Handbook*, Prentice-Hall, Upper Saddle River, NJ, USA, 1973.

[40] G. A. Milliken and D. E. Johnson, *Analysis of Messy Data, Analysis of Messy Data*, pp. 1206-1207, Chapman and Hall, CRC, CA, USA, 1992.

[41] U. Meier, "A note on the power of Fisher's least significant difference procedure," *Pharmaceutical Statistics*, vol. 5, no. 4, pp. 253–263, 2006.

[42] J. W. Geng, L. H. Li, and B. Tian, "Study on effect of viscosity reducer on rheological behavior and pumpability of concrete mixture," *journal of Highway and Transportation Research and Development*, vol. 8, 2017.

[43] J. F. Li and X. H. Huang, "The dispersion of lignin water reducing agent on cement raw slurry," *Journal of Guizhou University of Technology: Natural Science Edition*, vol. 30, no. 3, pp. 79–81, 2001.

[44] J. F. Li, "Research on water-reducing mechanism of modified lignosulfonate water-reducing agent for wet cement raw slurry," MS thesis, Guizhou University of Technology, Guiyang, China, 2001.